Pergamon

Int. J. Heat Mass Transfer. Vol. 38, No. 14, pp. 2677–2687, 1995

0017-9310/95 $9.50+0.00

0017-9310(94)00325-4

Heat transfer in a channel with a counter-current wall jet injection

E. P. VOLCHKOV, V. P. LEBEDEV, M. I. NIZOVTSEV and V. I. TEREKHOV

Institute of Thermophysics, Siberian Division of the Russian Academy of Sciences, Novosibirsk 630090, Russia

(*Received* 6 *June* 1994)

Abstract—In this work we present the results of an experimental investigation of heat transfer with a counter-current wall jet injection towards a main flow. In the experiments we studied heat transfer from a place of injection to the wall turn and downstream behind the place of injection. The investigation of an aerodynamic structure of a flow showed that the interaction of a jet with a counter-current flow resulted in the formation of a recirculation flow zone, and the heat transfer distribution had the same salient features, characteristic to separation flows. The formation of a new boundary layer behind the recirculation zone occurs under conditions of high-intensity external turbulence and the presence of a main flow velocity gradient. Consideration of these salient features leads to good agreement of the calculated and the experimental data on heat transfer. It has been shown that a velocity increase of the injected jet results in heat transfer increase, both in the area from the place of injection to the jet turn and downstream behind a place of counter injection. It has been established that heat transfer regulation within a broad range of parameters may be carried out by means of a jet injection.

1. INTRODUCTION

Investigating a heat exchange between liquid and gas flows and solid surfaces, many of researchers note the intensification of heat and mass transfer, which is conditioned by separation and subsequent re-attachment of a flow to a surface which is associated with considerable turbulization of the flow, and the presence of intensive recirculation flow zones etc. There are a great number of works that study the influence of different types of shoulders, fins and steps [1–4], abrupt restriction or expansion of passage cross-section of working channels [5, 6], the presence of diaphragms in tubes [7, 8] or of bodies with poor wind shape [9] on heat transfer. As numerous investigations showed, in such cases heat transfer is not uniform throughout a surface, and there are areas with its considerable increase. The heat transfer intensification degree may be determined by both the geometrical dimensions of the elements, disturbing a flow, and by the dynamic characteristics of a gas or liquid flow.

The elements disturbing a flow may be used to arrange highly efficient heat transfer. However, in this case, when a cooling flow rate is constant, it is pretty hard to regulate heat transfer because of necessity of change in the geometrical shape of the channels or the individual elements of a flowing part.

It is possible to increase heat transfer in a channel between a flow and a surface with the aid of a local jet injection. With this, it is quite easy to control the intensity of heat transfer by varying the flow rate of the injected jet. In refs. [10–13] it was shown that a jet injection at an angle with a surface may result in the flow separation from the channel surface. In this case the local heat transfer coefficients have a similar kind of distribution, as in the case of different disturbing elements in a flow or on a surface.

In refs. [14–16] we established that the regulated separation of a flow from a surface can be efficiently performed by means of a wall jet injection towards a main flow. A counter-current wall jet that develops in a restricted channel may considerably affect the average and pulsation characteristic of the flow, which in many respects determines the heat transfer processes between the flow and the channel wall.

There are only a limited number of works dedicated to counter-current wall jets. The review is given in ref. [19]. In ref. [17] the experimental investigation of some aerodynamic characteristics, such as the depth of a wall jet penetration to counter flow and distribution of pressure on a channel surface, is presented. The investigation of a counter-current wall jet effect on heat transfer between a flow and solid surface hasn't yet been carried out, as far as we know.

In the given work we are going to present the results of the experimental study of a counter-current wall jet influence on heat transfer between a gas flow and a solid surface in a restricted channel. We are also going to describe the experimental data of some dynamic and thermal characteristics in the areas from the place of injection to the jet turn and downstream behind the place of counter injection.

2. EXPERIMENTAL SETUP AND TECHNIQUE, MEASUREMENT EQUIPMENT

A scheme of the investigated flow is shown in Fig. 1. The experiments have been carried out in an aero-

NOMENCLATURE

a	temperature conductivity of air
A	coefficient in the heat transfer law, equation (9)
c_p	air heat capacitance
h	height of a channel
K	constant in the heat transfer law, equation (9)
l	long range of a jet
m	parameter of injection, $\rho_s u_s/\rho_0 u_0$
Nu_m	local Nusselt number in the point of a flow reattachment to the channel wall, $\alpha_m h/\lambda$
Pr	Prandtl number, ν/α
q	density of a heat flow on the wall
Re_T^*	Reynolds number, built from a thickness of energy loss, $u_0\delta_T^*/\nu_0$
Re	Reynolds number on the channel inlet, $u_0 h/\nu_0$
Re_s	Reynolds number calculated from initial jet parameters, $u_s h/\nu_s$
Re_x	Reynolds number, calculated from a length of an over-flowed surface $u_0 x/\nu_0$
$Re_{\Delta x}$	Reynolds number, determined from a coordinate Δx that is measured from a point of the boundary layer reattachment
s	height of a slot
St_0	Stanton number in a common boundary layer, $\alpha_0/\rho_0 u_0 c_p$
St_m	Stanton number, determined from the maximum velocity in a jet, $q_w/c_{p_0}(T_w - T_0)\rho_0 u_m$
St_s	Stanton number, determined from a velocity of the injected jet, $q_w/c_p(T_w - T_0)\rho_s u_s$
St^*	Stanton number in the area behind the point of the boundary layer reattachment, $q_w/c_{p_0}(T_w - T_0)\rho_0 u^*$
T_0	temperature in the flow core
T_w	temperature of a surface
T_s	temperature of air in the injected jet
T_u	turbulence intensity $(\sqrt{u'^2}/u_0)\cdot 100\%$
u_0	velocity in the flow core in the channel inlet
u_s	initial velocity of a counter-current jet
u^*	velocity in the flow core after a counter-current jet turn
u_m	maximum velocity in a wall jet profile
x	longitudinal coordinate, measured from a slot cross-section downstream
x'	longitudinal coordinate, measured from a slot cross-section towards the main flow
x_0	length of the initial part
Δx	coordinate, measured from a point of the flow reattachment
y	transverse coordinate.

Greek symbols

α	coefficient of heat transfer
δ	thickness of shear layer
δ_m	thickness of wall dynamic layer
δ_T	thickness of heat boundary layer
δ^*	thickness of displacement, $\int_0^{\delta_m}(1-(\rho u/\rho_m u_m))\,dy$
δ_T^*	thickness of energy loss, $\int_0^{\delta_m}(\rho u/\rho_m u_m)(1-\theta)\,dy$
λ	coefficient of heat conductivity
ν	kinetic viscosity of air
ρ	density of air
θ	non-dimensional temperature in a boundary layer $(T-T_0)/(T_w-T_0)$
Ψ	function of current, $\int_0^y u\,dy/u_0 h$
ψ	temperature factor, T_w/T_0
Ψ_{T_u}	heat transfer function, describing the influence of the elevated turbulence.

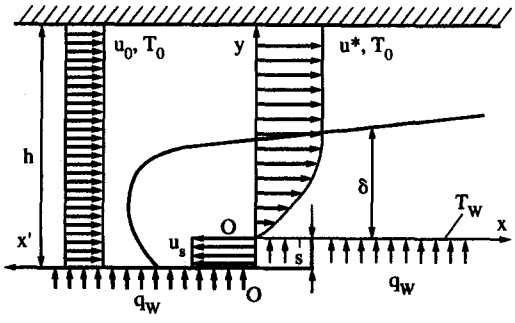

Fig. 1. Scheme of a counter-current wall jet flow.

dynamic tube of an open type with a working channel of rectangular cross-section 145 × 150 mm, with a length 1200 mm through which an air flow, with a velocity u_0 and a turbulence degree of $Tu_0 = 5\%$ flowed. On the lower surface of the working channel at a distance of 520 mm from the inlet we placed a slot injection chamber, with a slot height of $s = 8$ mm to form a counter-current wall jet with a velocity u_0.

The experiments have been carried out with following regime parameters. The velocity of the main flow was $u_0 = 12$ m s^{-1}, the Reynolds number was $Re_0 = u_0 h/\nu = 1.2 \times 10^5$. With this, when a counter-current jet at the place of the injection chamber

location was absent, there was a developed turbulent boundary layer with a thickness of displacement $\delta^* = 1.6$ mm and a form-parameter $H = \delta^*/\delta^{**} = 1.4$. The parameter of a secondary flow injection changed within a broad range of $m = \rho_s u_s/\rho_0 u_0 = 0.5$–12, and the Reynolds number of the secondary flow was $Re_s = u_s s/\nu_s = 3.3 \times 10^3$–$6.5 \times 10^4$. Temperatures of the main flow and a counter-current jet were equal during the experiments, and they were equal to the environmental temperature $T_0 = T_s = 288$–293 K. Density of heat flow on the channel surface was $q_w = 2400$ W m^{-2}.

In the experiments on the investigation of heat transfer, a heat flow was directed from the channel wall to the air flow. To reduce the heat leakages and increase the accuracy of experimental determination of local heat transfer coefficients compared with the traditional methods, we developed a special method of wall heating [18]. The essence of the method is as follows. On a working surface of a glass–textolite channel wall we spread an even layer of liquid coating made of graphite and soot with polymer binder. The uniformity of the coating thickness was provided by special gages. Then, the coating was carefully dried. The end of the drying process was determined by the stabilization of ohmic resistance of the coating. As a result, a thin electroconductive film with a thickness ~40 mm was formed on the wall. While the current passage film was heated, we could determine the density of heat flow q_w from the measured power. Since the film had an uniform thickness and heat transfer, the boundary condition $q_w = \text{const.}$ was valid on its surface.

Due to the low thermal conductivity the walls of the working channel, and of the thin electroheated layer, the longitudinal leakages of heat are small, which is of particular importance in the case of temperature gradients that took place in the direction of the longitudinal axis of the channel. The calibration measurements showed that heat leakages along the heated surface didn't exceed 0.3%. Heat leaks from the heat transfer coating were determined experimentally and constituted less than 5% of a total heat flow during experiments.

The heat transfer coefficients were found from the relationship

$$\alpha = q_w/(T_w - T_0). \tag{1}$$

The heat flow q_w regulation was carried out by changing the alternative current voltage which was fed through the copper busbars to the current conductive coating. The surface overheat with respect to the main flow did not exceed 50°C, so the maximum value of a temperature factor was $\psi = T_w/T_0 = 1.17$, and the flow might be considered to be quasi-isothermal. The wall temperature T_w was measured by chrome–copal thermocouples with a thickness of 0.2 mm. They were placed along the central line flush with the surface. The thermocouples were put on the working wall of the channel before spreading the heat transfer coating. To reduce heat leaks along the thermocouples wires, the electrodes, radiating from a thermocouple junction, were placed along the lines of isotherms. The length of the heat transfer part from the place of injection towards the main flow (in the direction of the axis Ox'—Fig. 1) amounted to 400 mm, and a width—120 mm. There were 40 thermocouples on this part. The heat transfer part behind the place of injection (Ox direction) had the same geometrical dimensions and number of thermocouples.

The utilized method of the heat transfer coefficient determination was evaluated during experiments on heat transfer between a heated plate and a non-compressed quasi-isothermal air flow. The heat transfer coefficients, measured in these standard conditions with an error of not more than 10%, were described by famous dependence for a developed turbulent boundary layer [20] with a constant heat flow on the wall

$$St_0 = 0.0306 Re_x^{-0.2} Pr^{-0.6}. \tag{2}$$

The measurements of temperature fields of the air flow were conducted by a thermocouple probe, with a junction diameter of 0.2 mm which was moved in the vertical direction by a computer-controlled coordinate device with a minimum shear step of 0.01 mm. As the preliminary experiments showed, during a wall jet interaction with counter flow, the considerable pulsations were observed. Thus, to obtain the reliable mean temperature values we should have averaged the measured signal over quite a long period of time. During the experiments the signal from the thermoprobe entered the device for data collection and processing, and at each point 500 measurements of temperature were performed for the time interval of 10 s.

The investigation of aerodynamics of a wall jet interaction with a running flow was performed by a two-component laser–Doppler anemometer. As a source of radiation, we used a LG-79 laser with power 15 mW and a length of wave $\lambda = 0.63$ mkm. The optical part of a velocity meter was made according to the differential three-beam scheme with a frequent separation of orthogonal components of the velocity vector. The electronic part involved a tracking system that allowed the extraction and processing of a Doppler signal. To obtain a Doppler signal, containing the information about a quantity and direction of velocity in the considered point, we injected the solid particles of silicon oxide with a dimension ~5 mm into a counter-current wall jet. The small dimensions of the particles provided good tracking behind the air flow.

The signal from the electronic part of laser–Doppler velocity meter entered the system of data collection through an Electronica-60 microcomputer to a SM-4 computer, where the whole experimental data processing was carried out. A more detailed description of optical and electronic equipment of the laser–Doppler velocity meter and its measurement error is given in ref. [21].

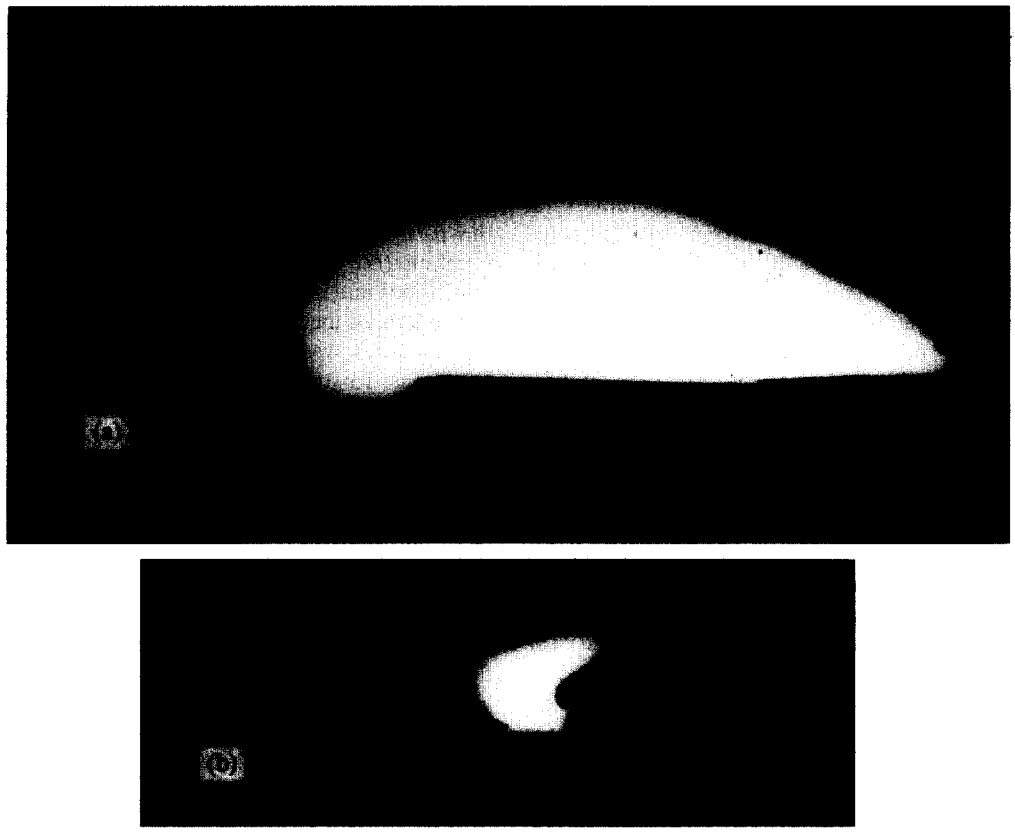

Fig. 2. Visualization picture of a counter-current wall jet flow. Injection parameter $m = 0.9$. (a) General picture of a flow; (b) picture of a flow after extraction the parts with the increased density of image.

The experimental program involved the visualization of a flow picture. The visualization of a flow was performed by a light knife method. Particles of cigarette smoke or powder with dimensions less than 1 mkm were injected into a wall jet. The lighting was conducted by a powerful plane pulse source of light, and the simultaneous photo recording of the interaction process was performed through side transparent channel walls. Such experiments allowed the determination of a long range of counter-current wall jet, as well as the height of the jet and flow mixture zone at different values of the injection parameter.

3. RESULTS OF A FLOW STRUCTURE DETERMINATION

The visualized picture of the counter-current wall jet flow is shown in Fig. 2. As is seen, an area of jet interaction with a running flow represents an extended cloud (see Fig. 2a). Density of the given image is not homogeneous, and if we extract more dense parts, we may obtain the picture of the flow which is shown in Fig. 2b. As can be seen from the photograph, when a counter-current wall jet leaves the injection chamber at a distance from the place of injection, it begins to diverge from the lower wall of the working channel, turns back and is removed by the running flow.

Similar visualized pictures were obtained for different values of the injection parameter which enabled us to track the change of geometrical dimensions of the zone of the jet and a counter flow mixing. These pictures were used for the quantitative findings of the jet penetration depth and the height of the mixture zone. The geometrical characteristics of the mixture area, which were determined according to the photographs, were close to the results obtained from measurements of velocity fields and temperatures.

The transformation of the velocity vector longitudinal component profile along the channel length is demonstrated in Fig. 3. We may note the complex character of the longitudinal velocity profile change. At a long distance from the injection place up-stream, the longitudinal velocity profile is pretty uniform with negligible thickness of the boundary layer near the channel wall (at $x'/s = 30$). As we approach the counter injection part, the longitudinal velocity profile becomes less filled (at $x'/s = 12.4$).

Then comes an area where the velocity at the wall changes its sign to the opposite. This area corresponds to the counter-current wall jet flow, therefore the velocity value as it approaches the slot cross-section increases from zero in the point of the jet retard up to the maximum value at the place it flows out of the slot (at $x'/s = 6.5, 5, 3$). The main flow in this area is over the zone of the counter jet turn, with this it increases its own velocity.

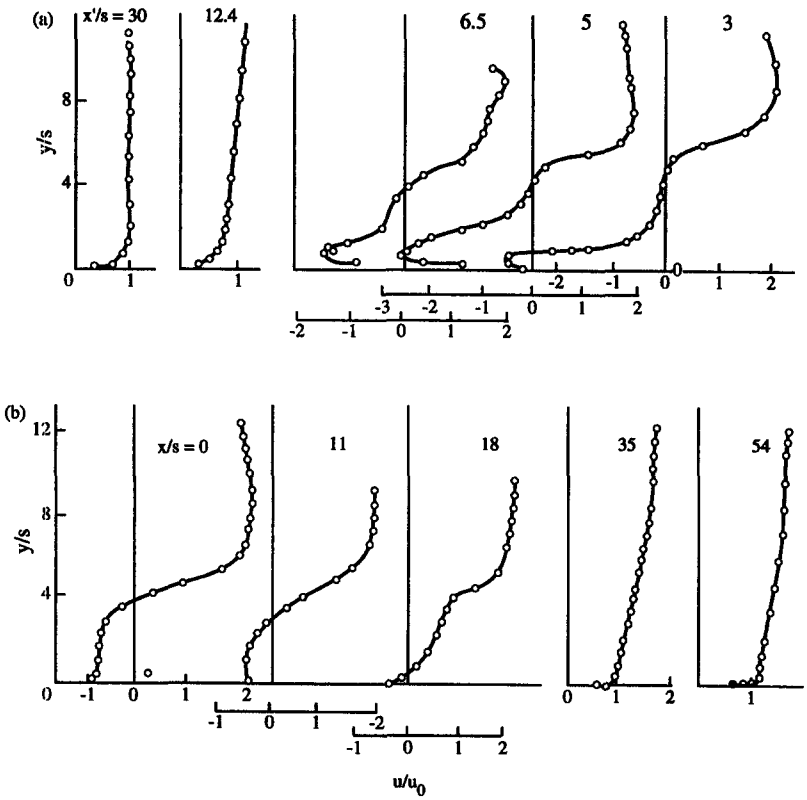

Fig. 3. Profiles of longitudinal velocity vector component at $m = 3$.

Directly behind the part of a counter injection the area of return flow is formed (at $x/s = 0$, 11, 18), its height gradually decreasing along the channel length. The reattachment of the shear layer of mixing to the lower channel wall, its further development and the formation of the new wall boundary layer take place downstream (at $x/s = 35$, 54).

The picture of the flow is more evident in Fig. 4 where there are lines of equal values of the current Ψ function of the investigated flow at the injection parameter $m = 3$. The current function values were determined by integrating the longitudinal velocity profiles $\Psi(y) = \int_0^y u\,dy/u_0 h$. With this, the velocity sign, coinciding with the main flow direction, was considered to be positive. The line of current $\Psi = -0.16$ in Fig. 4 restricts the area of the closed circulation flow. Behind this area the reattachment of the flow to the channel wall occurs. All distinctions of the counter-current jet interaction with the main flow which are marked in Figs. 2 and 3, may be observed in Fig. 4.

Further, we are going to consider the change of the most important dynamic characteristics of the flow which determine the heat transfer processes.

The change of the maximum velocity in the wall jet as it approaches the flow with different injection parameters is shown in Fig. 5. As it follows from the picture, the wall jet retards quite quickly due to the intensive process of mixing with the counter flow. At $m < 3$ the jet actually has no initial part where $u_m/u_s = 1$. At big injection parameters the initial part begins evidently extracting, its extent depending on the jet and the main flow velocity ratio. With the injection parameter m growth, a length of the initial part of the counter-current wall jet increases and strives within the limit of the length of the initial part of the submerged jet.

Behind the initial part there is a flow area where the longitudinal maximum velocity in the counter-current flow jet decreases from u_s to zero. According to the experimental data on this main part of the flow, the maximum velocity change may be taken from the linear dependence

$$\frac{u_m}{u_s} = 1 - \frac{x' - x'_0}{l - x'_0} \tag{3}$$

where l is dynamic long range of the counter-current wall jet. The long range characterizes the jet penetration depth to the running flow, and it may be determined according to the technique that was proposed in the work [14].

The wall jet turn, the foundation of a recirculation flow region which is flowed over the zone by the main flow, results in the significant change of velocity in the flow core. As it follows from Fig. 6, where we presented the velocity change along the channel in a flow

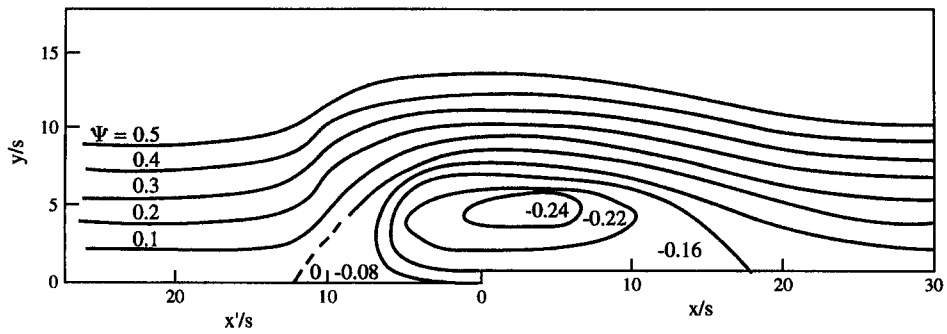

Fig. 4. Lines of equal values of the current functions with a counter-current jet injection ($m = 3$).

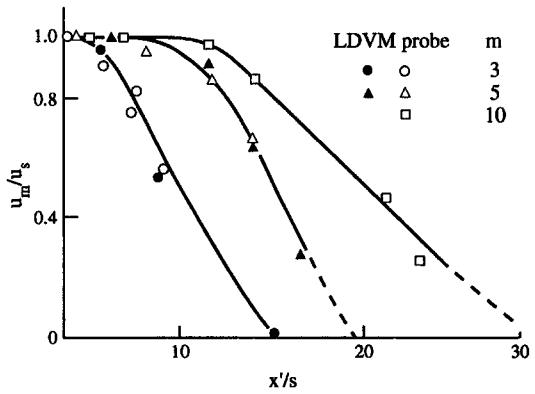

Fig. 5. Change of the maximum velocity in a counter-current wall jet.

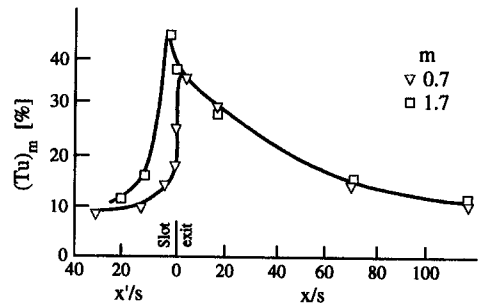

Fig. 7. Change of the maximum turbulence degree along the channel wall.

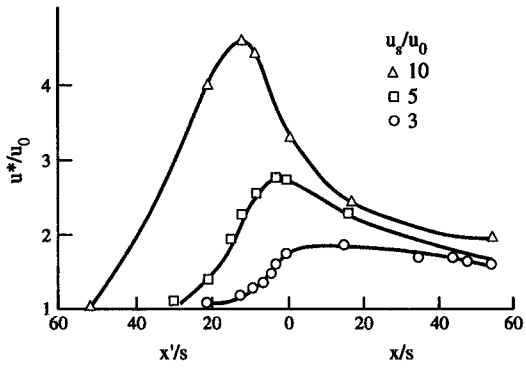

Fig. 6. Velocity increase in the flow core.

core during the experiments, the sub-compression of the flow resulted in increase of the value u^*/u_0 by more than four times. Let us also note the fact that, behind the point of flow reattachment to the channel wall ($x/s > 20$), the tempo of drop u^* abruptly decreased and for $10 < m < 3$ insignificantly differed from $u^*/u_0 \approx 2$.

The wall jet interaction with the counter flow, its turn and formation of the circulation zone result in the considerable turbulization of the flow. This follows from Fig. 7, where we showed the change of the maximum turbulence degree along a length of the channel. As is seen, the biggest value of the pulsation velocity was observed right in the vicinity of the jet injection place, where the turbulence degree may exceed 40%. The turbulence intensity remains quite high for a long way downstream behind the injection place. The increase of the relative velocity of the jet injection results in the certain growth of the turbulence degree only in the area ahead of the slot cross-section, and behind the injection place it has a weak effect on the quantity Tu_m.

As the measurements showed [19], the transverse profiles of the turbulence intensity significantly change along the channel length. The layer of the jet and the running flow mixture, the separation of the flow and the newly forming wall layer behind the flow reattachment point significantly influence on the formation of pulsation velocity fields. Correspondingly, the distinctions of the turbulent structure of the considered flow affect the processes of the turbulent heat transfer.

4. EXPERIMENTAL DATA ON HEAT TRANSFER

The distribution of local relative coefficients of a heat transfer α/α_0 in the area from the injection place to the counter-current wall jet turn at different injection

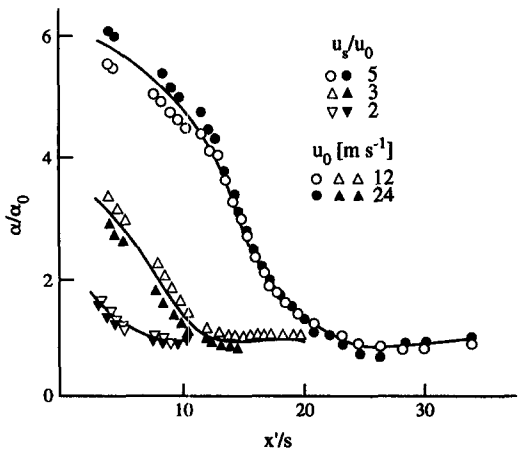

Fig. 8. Distribution of relative heat transfer coefficients in the area of a counter-current wall jet propagation.

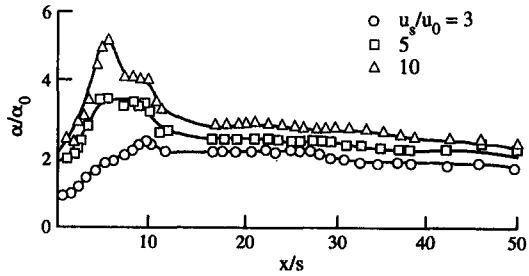

Fig. 9. Change of a relative coefficient of heat transfer behind the part of a counter injection.

intensities is shown in Fig. 8. The quantity α is the heat transfer coefficient at the jet injection, and α_0 is the heat transfer coefficient at the same point but without injection.

As it follows from the picture, the wall injection intensifies heat transfer in the area of the counter-current jet propagation. With this, the higher injection parameter m is, the greater increase of α occurs, and the more extended the zone of elevated heat transfer becomes. When removed from a slot cross-section the α/α_0 ratio gradually decreases to 1, and then the counter wall injection stops affecting the heat transfer, and it is described by the common dependence for the turbulent boundary layer. Such a fast decrease of the heat transfer coefficient as a jet penetrates the flow is conditioned, first of all, by an intensive retard of the jet by the running flow. You may see for yourself if you look at Fig. 5 where there is attenuation of the maximum velocity in a wall jet.

The experimental data, obtained at different absolute values of velocities of the jet and the non-disturbed flow but at the same values of the injection parameter, $m = u_s/u_0$, coincide. This confirms the independence of the relative heat transfer coefficient in that flow area on the absolute values of velocities of the jet and the flow at their constant ratio. According to the experimental data [19] the quantity of the maximum heat transfer coefficient within the range of injection intensities $1 < m < 10$ is determined by the simple dependence $\alpha_m/\alpha_0 \approx m$.

Let us get down to the analysis of experiments on the investigation of heat transfer in the area behind the place of a jet injection downstream. In Fig. 9 you can see the change of the relative heat transfer coefficient along the channel length at different parameters of the jet injection. As is seen, the counter-current wall jet results in the intensification of heat transfer in this flow area. With this, as for the above considered zone ahead of the slot cross-section, the greater the injection parameter is, the greater the increase of heat transfer occurring between the channel wall and the gas flow.

The entire area of the heat transfer coefficient change behind the injection place may be conventionally divided into two. The first area is located immediately behind the injection chamber slot cross-section $0 < x/s < 15$. Here, the fast increase of the heat transfer coefficient up to the maximum value takes place, and then we may observe its relatively quick decrease down to the certain quantity that slightly changes along the channel length. The value of the maximum relative coefficient of a heat transfer grows along with the injection parameter. Thus, for $m = 3$ we have $\alpha/\alpha_0 = 2.3$ and for $m = 10$—$\alpha/\alpha_0 = 5.2$. We may also note that along with the growth of the injection parameter the position of the maximum coefficient of heat transfer moves upstream.

The second area corresponds to $x/s > 15$. In this flow area the heat transfer coefficient at a counter injection along the whole extent of the investigated part ($15 < x/s < 52$) significantly exceeds the heat transfer coefficient without injection and slightly decreases along the channel length.

Such a non-uniform distribution of local coefficients of heat transfer is associated with salient features of gas dynamics of the flow (Figs. 3, 4, 6). In the area of the recirculation flow which is limited by the line of current $\Psi = -0.16$ in Fig. 4 we can observe the heat transfer coefficient growth. Behind the area of separation the reattachment of the flow to the channel wall takes place and, correspondingly, in this area there is the maximum heat transfer with the wall.

Such an increase of local coefficients of heat transfer was observed during the investigation of the broad range of flows, associated with the separation and the subsequent reattachment of the flow. Thus, for example, a comparison of local Nusselt numbers changes during the diaphragm provision in the round tube [7] and behind the place of a counter injection shows [19] that in these cases the distribution has a similar character.

The flow that is released behind the counter injection place looks like that described in the literature flow, following the jet normal to the flow. A comparison of results of the present investigation with data of ref. [10] shows that both in the case of normal

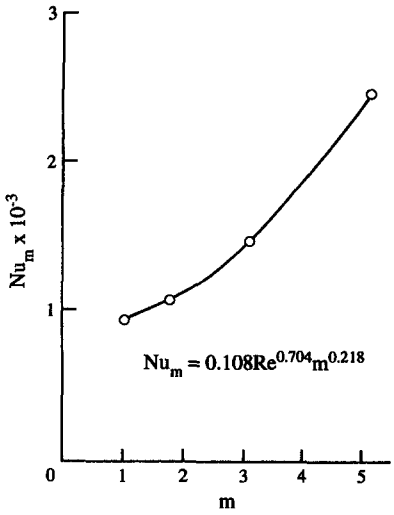

Fig. 10. Influence of the injection intensity on Nu_m behind the place of a counter and normal injection.

and the counter injections we may observe the peak-like distribution of heat transfer coefficients in restricted channels behind the injection place. With the increase of the injection gas flow rate in both cases we may see the growth of the maximum heat transfer coefficient and the maximum Nusselt number $Nu_m = \alpha_m h/\lambda$. The comparison of the experimental results of determination Nu_m for a counter injection with the generalizing dependence

$$Nu_m = 0.108 Re^{0.704} m^{0.218} \tag{4}$$

that was proposed in ref. [10] to generalize the experimental results on the normal slot injection shows (Fig. 10) that counter injection gives a maximum increase of heat transfer than does a normal injection at the same relative injection intensity, as well as the more significant growth of heat transfer with the increase of m.

The intensification of heat transfer processes behind the place of counter injection is confirmed by the experimental data on the investigation of transverse fields of mean temperatures. A comparison of non-dimensional temperature profiles in this area with and without the counter injection is given in Fig. 11. It is seen that the temperature profiles in the wall area where the basic processes take place which determine heat transfer between the channel wall and the gas flow are more filled at the jet injection compared to its absence. It confirms the intensification of heat transfer processes with the counter injection. At the same time the thickness of the heat layer for the case of the jet injection considerably exceeds the thickness of the layer without injection, and the temperature profile behind the recirculation zone is not actually changed at the counter injection along the channel wall on the entire investigated zone of the flow (to $x/s \approx 50$).

5. GENERALIZATION OF EXPERIMENTAL DATA ON HEAT TRANSFER

The development of the method for calculation of the flow and the turbulent heat transfer in the restricted channel with the counter wall injection represents a large problem. So the utilization of integral methods based on the experimentally grounded simplified assumptions is quite reasonable for these purposes.

The integral method for calculation of basic gasodynamic parameters of the considered flow was developed earlier in ref. [16]. Despite the utilization of certain assumptions the calculation results have good agreement with the results of the experimental investigations on the jet long range, a thickness of shear layer δ, a velocity value u^* in the flow core after a jet turn. The obtained calculated equations may also be used to determine heat transfer.

The analysis of heat transfer will be carried out as it was earlier made during experiments, i.e. individually for the area of the counter-current wall jet propagation along the channel wall up to its turn point and for the area from the injection place downstream of the main flow.

Let us make a calculation of heat transfer between the injected jet and the surface and, with this, we consider that the maximum velocity in the counter-current jet changes according to equation (3). For this reason we write down an integral equation of the boundary layer jet energy and assume that the thickness of wall dynamic and heat layers are equal:

$$\frac{d}{dx}[u_m \rho_0 c_p (T_w - T_0)\delta_T^*] = q_w. \tag{5}$$

Let us integrate this equation at $q_w = \text{const.}$ from x'_0 to x'.

$$(Re_T^* \Delta T)_{x'} - (Re_T^* \Delta T)_{x'_0} = \frac{q_w}{\rho_s u_s c_{p_s}} Re_s(\bar{x}' - \bar{x}'_0) \tag{6}$$

where $\bar{x} = x/s$.

Let us assume that on the initial part ($0 \leqslant \bar{x}' \leqslant \bar{x}'_0$) the heat transfer is described by the dependence for the boundary layer with the constant velocity on the exterior boundary. Consequently,

$$(Re_T^* \Delta T)_{\bar{x}'_0} = \frac{q_w}{\rho_s u_s c_{p_s}} Re_s \bar{x}'_0 \tag{7}$$

after the substitution of equation (7) into equation (6) we obtain

$$Re_{T\bar{x}'}^* = St_m Re_s \frac{u_m}{u_s} \bar{x}'. \tag{8}$$

Let us take a heat transfer law in a power form [20]

$$St_m = A Re_T^{*-k} Pr^{k-1}. \tag{9}$$

The joint solution of equations (8) and (9) gives an expression for calculation of the heat transfer coefficient

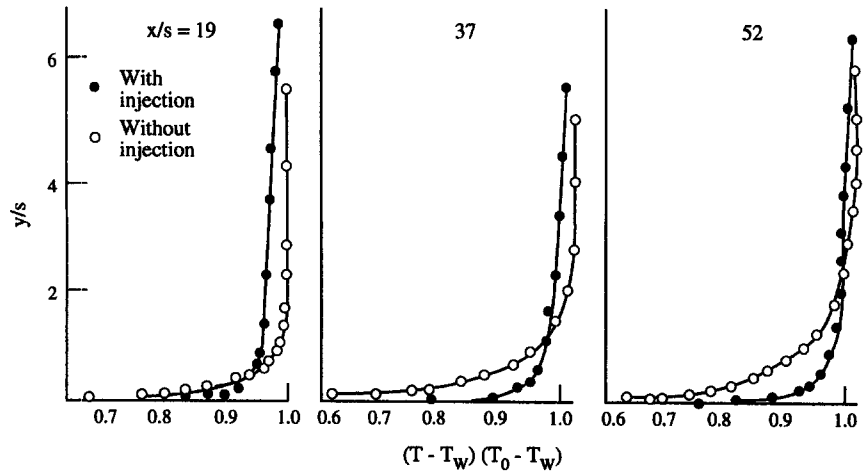

Fig. 11. Temperature profiles behind the recirculation zone.

$$St_m = A^{1/(k+1)} Re_s^{-k/(k+1)} \bar{x}'^{-k/(k+1)} \left(\frac{u_m}{u_s}\right)^{-k/(k+1)} \times Pr^{k-1/(k+1)}. \quad (10)$$

For a developed turbulent boundary layer with an index 1/7 in a power profile of velocity and temperature the constants in equation (10) are equal: $A = 0.0128$, $k = 0.25$. Having these values of A and k the equation (10) will be written down as follows:

$$St_s = 0.0306 Re_s^{-0.2} \bar{x}'^{-0.2} \left(\frac{u_m}{u_s}\right)^{0.8} Pr^{-0.6}. \quad (11)$$

When we substitute equation (4) for equation (11) we obtain a relationship for calculation of heat transfer on the main part of a counter-current wall jet

$$St_s = 0.0306 Re_s^{-0.2} \bar{x}'^{-0.2} \left(1 - \frac{x' - x_0}{l - x_0'}\right)^{0.8} Pr^{-0.6}. \quad (12)$$

The experimental data on heat transfer of the counter-current wall jet with the surface are presented in Fig. 12 for different injection intensities. Here, we show the calculation curves, obtained from the relationship (12) for corresponding parameters of injection. The long range of the jet l is determined from calculated dependencies of ref. [16]. As is seen from Fig. 12 there is good agreement between the calculated data and the experimental results. In the picture we may also see the calculated dependencies from relationship (10) for the heat transfer in the turbulent boundary layer with a constant velocity on its exterior boundary ($u_m = u_s$) and in a submerged wall jet where the velocity drop tempo was described by the relationship, proposed by Seban and Back [22].

$$u_m/u_s = 3.6(x'/s)^{-0.45}. \quad (13)$$

As is seen the decrease, tempo of heat transfer along the channel length in the boundary layer with a constant velocity on its exterior boundary and in the submerged wall jet is significantly slower than in counter-current jets.

Besides, we should note that it is reasonable to perform the calculation of the counter-current wall jet heat transfer on the main part of the jet development in the area from x_0 to $(0.7–0.8)l$. At longer distances from the injection place the maximum velocity significantly decreases, and the jet long range pulsations, observed in the experiment, begin influencing the heat transfer intensity. With this, the given calculation technique ignores these features of the flow.

Let us generalize the experimental data on heat transfer behind the recirculation flow zone at the counter wall injection.

The basic factors, resulting in the heat intensification behind the point of a shear layer reattachment to the channel surface, are the increase of velocity in the flow core u^* (Fig. 6) and the intensity of turbulent flow pulsations (Fig. 7). In this connection, during generalization of the experimental data on heat transfer we took into account the increase of the flow velocity and the turbulent level. With this, the Stanton numbers and the Reynolds numbers were determined

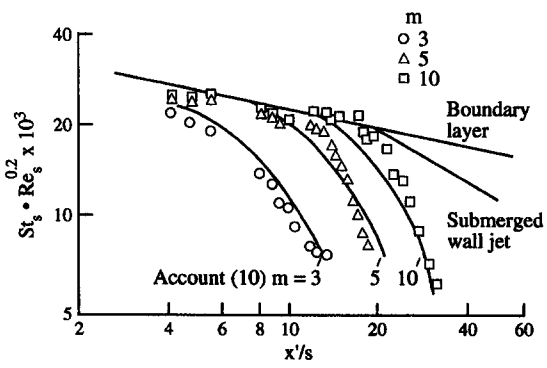

Fig. 12. Heat transfer of a counter-current wall jet on the basic part of its development.

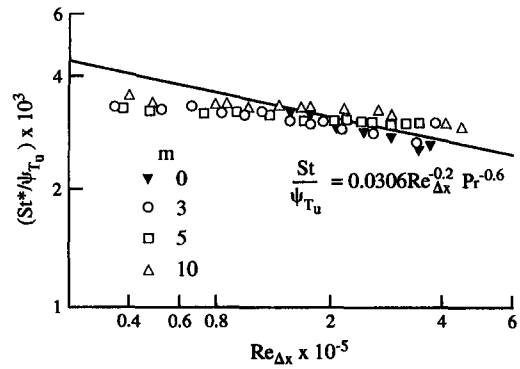

Fig. 13. Generalization of experimental data on heat transfer behind the recirculation zone.

as $St^* = \alpha/\rho_0 u^* c_{p_0}$ and $Re_{\Delta x} = \rho_0 u^* \Delta x/\mu_0$ where the distance Δx was measured from the start of the heat boundary layer formation (from the point of the shear layer reattachment to the channel wall). The influence of the elevated turbulence was considered with the aid of the relative heat transfer function [23].

$$\Psi_{T_u} = St^*/St_0 = (1+0.0085)^{0.8} \qquad (14)$$

where St_0—Stanton number in the low-turbulent flow and $T_u = (\sqrt{u'^2}/u^*)100\%$—degree of turbulence on the exterior boundary of the boundary layer.

The results of the performed generalization are shown in Fig. 13 in the form of dependence $St^*/\Psi_{T_u} = f(Re_{\Delta x})$. It is seen that in such processing the experimental data, obtained for different injection parameters, generalize with each other. To compare, we presented the calculation of heat transfer in the standard turbulent boundary layer according to equation (2) on the same scheme.

The experimental data are in quite good agreement with the calculations according to this equation. The fluctuation of experimental points from the curve may be conditioned by discarding the dynamic prehistory of the flow, as well as by formation of the large-scale turbulent structure of the flow which appears as a result of the interaction of the counter-current jet with the flow. Even in the first approximation of the jet in the restricted channel behind the point of reattachment of a shear layer of mixing, it may be described by the dependence of the common turbulent boundary layer, if we consider the velocity increase in the flow core and the turbulent level growth.

6. CONCLUSIONS

The experimental study of the counter-current wall jet influence on heat transfer between an air flow and the solid surface in a restricted channel showed:

(1) A counter-current wall jet leads to local heat transfer intensification in the area from the place of injection to the jet turn zone. With this, the length of the elevated heat transfer area and a quantity of the heat transfer growth may be regulated by the intensity of the counter-current injection.

(2) In the restricted channel the counter-current wall jet may increase heat transfer between the channel wall and the gas flow by 2–3 times along the whole investigated extended part behind place of injection (in the experiments it was up to $x/s = 50$).

(3) A complex character of distribution of local heat transfer coefficients along the channel length behind the place of counter-current injection is determined by the flow aerodynamics, i.e. by phenomena of separation and reattachment of the flow to the surface, by the presence of the recirculation flow zone and by the considerable turbulization of the flow by the counter-current jet.

(4) Heat transfer of the counter-current wall jet to the channel wall on the basic part of its development from the place of injection to the turn zone is described by the dependence (12) that was obtained from the solution of the integral equation of energy for the wall boundary layer of the counter-current jet.

(5) Heat transfer behind the recirculation flow zone with the counter-current wall injection may be described in the first approximation by the dependence for the common turbulent layer (2) if we take into account the increase of velocity and the turbulence degree in the flow core.

REFERENCES

1. N. Seki, S. Fukusako and T. Hirata. Turbulent fluctuations and heat transfer for separated flow associated with a double step at entrance to an enlarged flat duct, *J. Heat Transfer* **98,** 581–587 (1976).
2. J. C. Vogel and J. K. Eaton, Combined heat transfer and fluid dynamic measurements downstream of backward-facing step, *J. Heat Transfer* **107,** 922–925 (1985).
3. J. K. Eaton and J. P. Johnston, A review of research on subsonic turbulent flow reattachment, *AIAA J.* **19,** 1093–1100 (1981).
4. A. I. Gnyrya, V. I. Terekhov, S. P. Tretyakov and N. I. Yaryguina, Heat transfer by forced convection from a heated surface in a cavity, formed by two high fins, *Z. prik. mekh. tekh. fisi.* **N3,** 103–108 (1993).
5. J. W. Baught, M. A. Hoffman, R. K. Takanashi and B. E. Launder, Local heat transfer downstream of an abrupt expansion in a circular channel with constant wall heat flux, *J. Heat Transfer* **106,** 789–796 (1984).
6. A. Garcia and E. M. Sparrow, Turbulent heat transfer downstream of a constraction-related, forward-facing step in duct, *J. Heat Transfer* **109,** 621–626 (1988).
7. K. M. Krall and E. M. Sparrow, Turbulent heat transfer in the separated, reattached and redevelopment regions of a circular tube, *J. Heat Transfer* **88,** 145–152 (1966).
8. E. K. Kalinin, G. A. Dreitser and S. A. Yarkho, *Intensification of Heat Transfer in Channels*, c.206. Mashinostroenie, Moscow (1981).
9. T. Ota and N. Kon, Turbulent transfer of momentum and heat in a separated and reattached flow over a blunt flat plate, *J. Heat Transfer* **102,** 745–754 (1980).
10. S. Wittig and V. Scherer, Transfer measurements downstream of two-dimensional jet entering a crossflow, *J. Turbomachin.* **110,** 572–578 (1987).
11. R. C. Foster and A. Haji-Sheikh, An experimental investigation of boundary layer and heat transfer in the region of separated flow downstream of normal injection slots, *J. Heat Transfer* **97,** 260–266 (1975).

12. D. K. Mukherjee, Film cooling with injection through slots, *J. Eng Power* **98,** 556–559 (1976).
13. E. M. Sparrow and R. G. Kemink, The effect of mixing tee on turbulent heat transfer in tube, *Int. J. Heat Mass Transfer* **22,** 909–917 (1979).
14. V. P. Lebedev and M. I. Nizovtsev, Thermal characteristics of a counter-current wall jet, *J. Appl. Mech. Tech. Phys.* **30,** 776–779, (1989).
15. E. P. Volchkov, V. P. Lebedyev, M. I. Nizovtsev and V. I. Terekhov, Heat transfer in a channel behind the parts of a counter-current wall jet injection, *Izvestia SO AN SSSR Ser. Tech. Sci.* **3,** 21–25 (1990).
16. V. P. Lebedev, M. I. Nizovtsev and V. I. Terekhov, Spreading of boundary jet in a counter flow, *J. Appl. Mech. Tech. Phys.* **32,** 231–235, (1991).
17. R. Balachander, L. Robillard and A. Romamurthy, Some characteristics of counter flowing wall jets, *J. Fluid Engng* **114,** 554–557 (1992).
18. E. P. Volchkov, V. P. Lebedev and A. N. Yadykin. Heat transfer by unbalanced flow with a screen in the Laval nozzle, *Heat Transfer VI: Proc. of VI All-Union Conf. Heat and Mass Transfer, Part* 2, vol 1, pp. 44–49, Minsk (1987).
19. M. I. Nizovtsev, Interaction of a wall jet with a counter flow in a restricted channel, Dissertation for Ph.D. in technical sciences, 157 pp. Novosibirsk (1991).
20. G. Schlihting, *Theory of a Boundary Layer*, pp. 712. Nauka, Moscow (1974).
21. V. A. Gavrilov, E. V. Kozhukova, S. Yu. Spotar *et al.*, Automatic installation for studying turbulent vortex streams by a two-component anemometer, up-to-date experimental methods of studying the heat and mass transfer processes, *Int. School-Seminar*, Part 2, pp. 109–116, Minsk (1987).
22. R. A. Seban and I. H. Back, Velocity and temperature profiles in a wall jet, *Int. J. Heat Mass Transfer* **3,** 255–265 (1961).
23. V. N. Mamonov, Heat transfer on a permeable plate with the elevated degree of the running flow turbulence. In *Turbulent Boundary Layer under Complex Boundary Conditions*, Izd-vol. SO AN SSSR, pp. 60–72. Novosibirsk (1977).